FEBS Letters 569 (2004) 82–88 FEBS 28505

Localization of the Tat translocon components in *Escherichia coli*

Felix Berthelmann, Thomas Brüser*

Institute of Microbiology, University of Halle-Wittenberg, Kurt-Mothes-Str. 3, D-06120 Halle, Germany

Received 15 March 2004; revised 17 April 2004; accepted 18 May 2004

Available online 7 June 2004

Edited by Stuart Ferguson

Abstract The Tat system has the ability to translocate folded proteins across the bacterial cytoplasmic membrane. In *Escherichia coli*, three functionally different translocon components have been identified, namely TatA, TatB, and TatC. These proteins were fused to the green fluorescent protein (GFP) and their localization was determined by confocal laser scanning fluorescence microscopy. TatA-GFP was distributed in the membrane, often with higher abundance at the poles. TatB-GFP was found in distinct spots at the poles of the cells. The fluorescence of TatC-GFP was very low and required a constitutive expression system to become higher than background, but then appearing polar. All three constructs complemented the chain-formation phenotype of corresponding mutant strains, indicating the functionality of the fusion proteins. TatB-GFP and TatC-GFP also complemented TMAO respiration deficiency and TatA-GFP the SDS-sensitivity of the mutant strains. The localization of the translocon-GFP fusions coincides with the fluorescence pattern of GFP fusions to Tat substrate signal sequences. We suggest that the active translocon complexes are mainly present at polar positions in *Escherichia coli*.

Keywords: Green fluorescent protein; Fusion protein; Twin-arginine translocation; TatABC complex localization; Protein transport

1. Introduction

The bacterial twin-arginine translocation (Tat) system can translocate folded proteins across the cytoplasmic membrane [1]. A homologous translocation machinery is present in plant thylakoid membranes [1]. In *Escherichia coli*, three functionally distinct components are known, TatA/E, TatB and TatC, all of which are essential for Tat dependent translocation [2]. TatE is a paralog of TatA, with overlapping function [3]. TatA/E and TatB are N-terminally membrane anchored and have hydrophilic C-terminal domains which face the cytoplasm, whereas TatC is predicted to span the membrane six times with both termini located in the cytoplasm [2].

Three distinct high molecular weight Tat complexes have been isolated so far: a 600 kDa TatAB complex [4], a 600 kDa TatABC complex [5], and a 460 kDa TatA complex [6]. Of these, only the TatABC complex appears to bind Tat substrates, suggesting that TatC is required for Tat-substrate binding [7]. This has recently been supported by in vitro cross-linking studies, which indicate that TatC is responsible for the initial contact of the translocation apparatus to the Tat substrate [8].

In order to find out where the Tat components are localized within the cells, we constructed and analyzed C-terminal translational fusions of TatA, TatB, and TatC with the green fluorescent protein (GFP), using differently regulated expression systems. TatA was distributed across the membrane, and in many cells the fluorescence was increased at the cell poles. TatB-GFP was present in distinct spots at the cell poles and only very little fluorescence was seen between those spots. TatC-GFP was detected in polar spots as well, however, TatC-GFP fluorescence was low and only detectable with a constitutive expression system. The fusion proteins were translocation competent, suggesting that transport takes place in mainly polar structures containing TatA, TatB and TatC.

2. Materials and methods

2.1. Strains and plasmids

Escherichia coli strain MC4100 [9], and its *tat* mutant derivatives JARV16 (MC4100 Δ*tatAE*) [10], BϕD (MC4100 Δ*tatB*) [10], and B1LK0 (MC4100 Δ*tatC*) [11] were used for localization and complementation studies. Arabinose resistant mutants from MC4100 and its derivatives were isolated on LB agar with 1% arabinose [12] and used for all experiments with arabinose-dependent gene expressions. *E. coli* XL1-Blue Mrf' Kan (Stratagene) was used for all cloning steps. Bacteria were grown aerobically at 37 °C on LB medium (1% tryptone, 1% NaCl, and 0.5% yeast extract) in the presence of the appropriate antibiotics (20 μg/ml chloramphenicol, 12.5 μg/ml tetracycline and 100 μg/ml ampicillin). TMAO respiration was tested by anaerobic growth on M9 medium supplemented with 0.8% glycerol, 1.1% TMAO, 1 μM Na_2SeO_3 and other trace elements (SL12, [13]).

The *tat* expression low copy vector pABS-*tatABC* (Table 1) was generated by cloning the *tatABC*-containing *Bam*HI/*Sac*I fragment of pRK-*tatABC* [14] into the *Eco*RV-site of pABS, a pACYC184 (Fermentas) derivative containing the *Hae*II excised pBluescript-SKII(+) multiple cloning site cloned into its single *Eco*RV site. For construction of the *tatA-gfp* and *tatB-gfp* fusions, the *Xho*I site in the vector was deleted by restriction, blunting and religation, followed by the introduction of a unique *Xho*I site in the 3′-end of *tatA* or *tatB* in pABS-*tatABC* using QuikChange™ (Stratagene) mutagenesis with the primers *tatA-Xho*I-F (5′-GCG CCA CGA TAA AGA GCT CGA GTA ATC CGT GTT TG-3′), *tatA-Xho*I-R (5′-CAA ACA CGG ATT ACT CGA GCT CTT TAT CGT GGC GC-3′), *tatB-Xho*I-F (5′-CAC CTT CCC CTT CGT CGC TCG AGA AAC CGT AAA CAT G-3′) and *tatB-Xho*I-R (5′-CAT GTT TAC GGT TTC TCG AGC GAC GAA GGG GAA GGT G-3′). The *gfp*-gene was amplified from pTB-DG (see below) with the *Xho*I-site introducing primers GFP-*Xho*I-F (5′-GCT AGC TGG AGC CAC CTC GAG TTC GAA AAA ATC G-3′) and GFP-*Xho*I-R (5′-GTC TGG CGC ATT TAT TTC TCG AGT TCA TCC ATG CCA TG-3′), restricted with *Xho*I, and introduced at

* Corresponding author. Fax: +49-34555-27010.
E-mail address: t.brueser@mikrobiologie.uni-halle.de (T. Brüser).

Abbreviations: Tat, twin-arginine translocation; GFP, green fluorescent protein; TMAO, trimethylamine N-oxide

0014-5793/$22.00
doi:10.1016/j.febslet.2004.05.054

Table 1
Survey of used strains and plasmids

Strain	Genotype	Source
XL1-Blue Mrf′ Kan	Δ(*mcrA*)*183* Δ(*mcrCB-hsdSMR-mrr*)*173 endA1 supE44 thi-1 recA1 gyrA96 relA1 lac* [F′ *proAB lacI*^{q}*ZΔM15* Tn*5* (Kan^{r})]	Stratagene
MC4100	F^{-} *araD139 lacU169 relA1 rpsL150 thi mot flb5301 deoC7 ptsF25 rbsR*	[9]
JARV16	MC4100, *ΔtatAE*	[10]
BϕD	MC4100, *ΔtatB*	[10]
B1LK0	MC4100, *ΔtatC*	[11]
Plasmid	**Insert/Characteristics**	**Source**
pABS	*Hae*II fragment with MCS of pBS-SKII+ cloned into *Eco*RV site of pACYC184, p15A origin, *cat*	This work
pABS-*tatABC*	*tatABC* under control of constitutive *tatA* promoter cloned into *Eco*RV site of pABS, *cat*	This work
pABS-*tatABCstrep*	pABS-*tatABC* with Strep-TagII from pASK-2 (IBA, Göttingen, Germany) at C-terminus of *tatC*, *cat*	This work
pABS-*tat*(*A-gfp*)*BC*	pABS-*tatABC* with *gfp* fused at C-terminus of *tatA*, *cat*	This work
pABS-*tatA*(*B-gfp*)*C*	pABS-*tatABC* with *gfp* fused at C-terminus of *tatB*, *cat*	This work
pABS-*tatAB*(*C-gfp*)	pABS-*tatABCstrep* with *gfp* fused at C-terminus of *tatC*, *cat*	This work
pBAD22	Vector for arabinose-regulated expression, *araC*, *araBAD*-promoter, *rrnB* terminator, pBR origin, *bla*	[31]
pBAD-*tatA-gfp*	*tatA-gfp* cloned into *Nco*I/*Xba*I sites of pBAD22, *bla*	This work
pBAD-*tatB-gfp*	*tatB-gfp* cloned into *Nco*I/*Xba*I sites of pBAD22, *bla*	This work
pBAD-*tatC-gfp*	*tatC-gfp* cloned into *Nco*I/*Xba*I sites of pBAD22, *bla*	This work
pTB-DG	Expression of *dmsA*(signal sequence)-Strep-TagII-*gfp* under control of P_{tac}, *bla*	This work

the *Xho*I-restricted 3′-ends of *tatA* or *tatB*. For construction of the *tatC-gfp,* a *Bgl*II site was introduced at the 3′-end of *tatC* in pABS-*tatABC* using the primers *Bgl*II-tatC-F (5′-GAA GCA GAA AGC GAA AGA TCT GAA GAA TAA ATT CAA CCG-3′) and *Bgl*II-tatC-R (5′-CGG TTG AAT TTA TTC AGA TCT TTC GCT TTC TGC TTC-3′) and the Strep-Tag II^{TM} containing *Bam*HI-*Sca*I fragment from pASK2 (IBA) was cloned into the 6280 bp *Bgl*II–*Ssp*I fragment from pABS-*tatABC*. The *Xho*I–*Xho*I *gfp* fragment was then cloned into the single *Xho*I site present in pABS-*tatABC-strep* at the 3′-end of *tatC-strep*.

Regulated expression of *tatA-gfp*, *tatB-gfp*, or *tatC-gfp* was achieved by cloning these fusion genes behind the arabinose controlled promoter of pBAD22. For that, the genes were amplified with the primers *Nco*I-*tatA-gfp*-F (5′-GGA ACA TCC ATG GGT GGT ATC AGT ATT TGG-3′), *Xba*I-*tatA-gfp*-R (5′-AGC AGT TCT AGA AAA CCG ATA TCA AAC ACG G-3′), *Nco*I-*tatB-gfp*-F (5′-TGT AAT CCA TGG TTG ATA TCG GTT TTA GCG AAC-3′), *Xba*I-*tatB-gfp*-R (5′-GTA TCT TCT AGA GAC ATG TTT ACG GTT TCT CG-3′), *Nco*I-*tatC-gfp*-F (5′-CCG TAA CCA TGG CTG TAG AAG ATA CTC AAC CG-3′), *Xba*I-*tatC-gfp*-R (5′-GCA GAC TCT AGA AAT GTC GCA CAA TGT GCG C-3′), restricted with *Nco*I and *Xba*I and cloned into the corresponding sites of pBAD22.

The gene fusion encoding the DmsA signal sequence, StrepTag II (IBA, Göttingen) and GFP expressed under control of the *tac*-promoter (pTB-DG) was constructed by substituting the cytochrome c gene cassette in a pCS906 derivative [15] with the *Nde*I/*Bam*HI excised GFP-coding region from a pKENGFPmut2 derivative [16], in which an internal *Nde*I site was deleted in-frame by a silent mutation. The nucleotide sequence of the HyaA signal peptide in this pCS906 derivative was replaced *Nco*I/*Nhe*I by that of the DmsA signal peptide. All constructs were confirmed by sequencing.

2.2. Biochemical and microscopic methods

For preparation of membranes, 0.5 g cells from aerobically grown cultures were resuspended in 5 ml ice cold 50 mM Tris acetate, pH 7.5, and disintegrated by sonification. Cell debris was removed by centrifugation (10′, 20 000 × *g*, 4 °C), membranes were sedimented by ultracentrifugation (1 h, 130 000 g, 4 °C) and resuspended in 0.5 ml of 50 mM Tris–acetate, pH 7.5. Protein estimations were done using the Lowry method [17], SDS–PAGE analysis was done by the Laemmli method [18], and for immunoblot analysis, gels were semidry blotted and blots were developed as described previously [19], using rabbit sera against TatA, TatB (Tim Yahr, Iowa, USA) or TatC (Matthias Müller, Freiburg, Germany). GFP-fluorescence was examined by confocal laser scanning microscopy using a Carl Zeiss Axiovert 100M/LSM510 setup with a C-Apochromat 63x NA1.2 W (water immersion) objective. Excitation was at 488 nm and emission was detected at 505–530 nm. Cells were visualized by differential interference contrast (DIC), using Nomarski optics unless otherwise indicated. Micrographs were captured with Zeiss LSM software. For microscopical analysis, exponentially growing cultures were analyzed in LB medium without concentration or dilution of the sample. Strains containing pBAD-derivatives were grown for 2–4 h in the presence of L-arabinose at indicated concentrations prior to analyses.To immobilize cells, slides were thin-coated with 2% agarose in LB medium.

3. Results

3.1. Localization of TatA-GFP, TatB-GFP, and TatC-GFP

We constructed translational *tatA*-, *tatB*-, and *tatC-gfp* fusions under control of the arabinose-regulated pBAD expression system (Table 1) and examined the localization of the respective Tat-GFP fusion proteins by laser scanning microscopy (Fig. 1).

When *tatA-gfp* was expressed in the wild type strain MC4100 and its *tatAE* deficient derivative JARV16, fluorescence could be readily detected which appeared like halos, indicating that TatA-GFP is present in the whole membrane (Fig. 1A (with inset) and C). Interestingly, many cells showed an increase of fluorescence towards the poles, suggesting that TatA is more abundant at the cell poles than at other positions.

When *tatB-gfp* was expressed in MC4100 or its *tatB* deletion mutant BϕD, the bacteria showed spots of fluorescence which almost always were present at the cell poles or at cell division planes (Fig. 1E and G). We found that TatB-GFP is restricted to those usually polar positions in the membrane and not homogeneously distributed, suggesting that TatB-GFP may not occur in significant amounts as a freely diffusing membrane protein – which would be in contrast to the distribution of TatA-GFP. We could not find any condition under which TatB-GFP was not polar.

TatC-GFP showed very low fluorescence and we could not obtain significant fluorescence at levels above the cellular background when we used the pBAD system with up to 0.5% arabinose as inductor (compare Fig. 1J with I). However, when the constitutive *tatA*-promoter was used and the *tatAB(C-gfp)* genes were expressed together from the plasmid pABS-*tatAB(C-gfp)*, we were able to detect fluorescence which was above background levels at the poles (Fig. 1K). We do not know at this stage, why *tatC-gfp* requires the variant

expression system for the production of detectable fluorescent protein. As a constitutive pABS-based *tat*-expression system was required for visualization of TatC-GFP, we suggest that the observed polar localization of TatC should only be considered as a first evidence which awaits further studies by other methods.

It has been shown that GFP, when fused to the signal sequence of TorA, is Tat-dependently translocated [20–22]. A halo is formed by periplasmic GFP and it has been recognized that the fluorescence is stronger at the cell poles [20,21]. This polar concentration of transported Tat substrates was also found when full length AmiA was fused with GFP [23]. We observed the same halo and polar concentration with a DmsA-GFP fusion protein (Fig. 1L and N). In a *tatC* deletion strain, DmsA-GFP was homogeneously distributed in the cytoplasm, confirming that the polar pattern depends on the presence of the Tat system (Fig. 1M). However, while Bernhardt and de Boer [23] speculate that the polar concentration of translocated GFP might be due to a thicker periplasm at the cell poles, the localization of TatA-GFP, TatB-GFP and TatC-

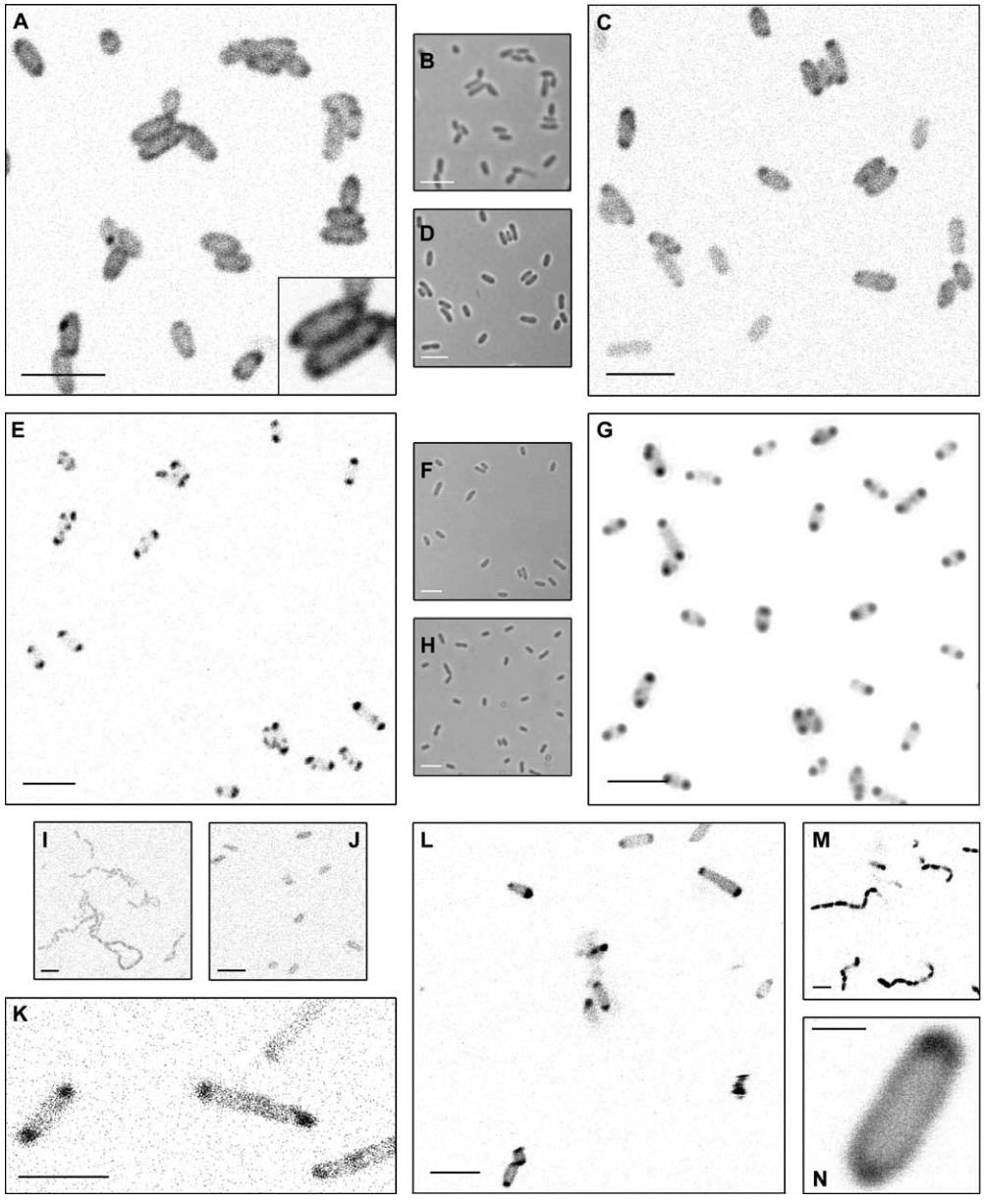

Fig. 1. Microscopic detection of GFP fusion proteins in *Escherichia coli*. Fluorescence and differential interference contrast microscopy was carried out as described in Section 2. Fluorescence is shown inverted and thus appears dark in the shown fluorescence micrographs. (A) A-GFP fluorescence in JARV16/pBAD-*tatA-gfp* (inset: enlarged detail showing the halo-like distribution of TatA-GFP); (B) cells from A; (C) A-GFP fluorescence in MC4100/pBAD-*tatA-gfp*; (D) cells from C; (E) B-GFP fluorescence in BΦD/pBAD-*tatB-gfp*; (F) cells from E; (G) B-GFP fluorescence in MC4100/pBAD-*tatB-gfp*; (H) cells from G; (I) autofluorescence of B1LK0/pBAD22 at maximum detection sensitivity; (J) fluorescence of B1LK0/pBAD-*tatC-gfp* at maximum detection sensitivity; (K) C-GFP fluorescence of B1LK0/pABS-*tatAB(C-gfp)*; (L) DmsA-GFP fluorescence in MC4100/pTB-DG; (M) DmsA-GFP fluorescence in B1LK0/pTB-DG; (N) DmsA-GFP fluorescence in MC4100/pTB-DG. The images (G) and (H) are whole cell fluorescence and phase contrast micrographs, respectively. pBAD-expression systems were either induced with 0.1% (A, B, E, F) or with 0.5% L-arabinose (C, D, G, H, I, J). Bars in the photos indicate 5 μm except of the bar in (N) which indicates 1 μm.

GFP suggests that the polar appearance of GFP Tat substrates may be a direct consequence of the mainly polar presence of the Tat translocon.

3.2. TatA-GFP, TatB-GFP and TatC-GFP fusions are functional

Having localized the Tat-GFP fusions within the bacterial cell, we approached the functionality of the GFP-containing translocons. Firstly, we confirmed by immunoblot analysis that TatA-GFP, TatB-GFP and TatC-GFP were present in the membranes of the respective strains as full length proteins with both used expression systems (Fig. 2). All Tat-GFP fusion proteins were produced and detectable. TatA and TatB appeared to be more abundant in the induced system, whereas TatC was hardly detectable in that system (Fig. 2B). The amount of fusion proteins was lower than that of unfused proteins expressed from pABS-*tatABC* (Fig. 2A), but still significantly higher than wild type level, as wild type level Tat components were not detectable with the used antibodies and the amount of protein analyzed (Fig. 2B). This observation was already made by others who used the same antibodies against TatA and TatB and who could detect only overexpressed Tat components in crude membranes [24]. The GFP domain of the Tat-GFP fusions has a molecular weight of 28 kDa. This is huge when compared to the molecular mass of the native Tat components, which is near 10 kDa (TatA), 18 kDa (TatB) and 29 kDa (TatC). Moreover, the functional Tat translocon is believed to consist of multiple copies of these components, thus multiplying the GFP-"appendices" at each individual translocon. Based on this, it is not self-evident that the Tat-GFP fusion proteins retain their function within the translocon. Nevertheless, the first evidence for functionality comes already from the microscopic analysis: strains without a functional Tat translocon cannot translocate two cell division amidases, AmiA and AmiC [23]. As a consequence, cells do not separate completely after division and a "chain formation phenotype" becomes evident. The *tatA/E* deletion strain JARV16 with TatA-GFP (Fig. 3C), the *tatB* deletion strain BϕD with TatB-GFP (Fig. 3F) and the *tatC* deletion strain B1LK0 with TatC-GFP (Fig. 3I) do not form cell chains, indicating that these GFP-fusions are assembled into functional Tat translocons. Interestingly, the levels of uninduced pBAD-*tatB-gfp* and pBAD-*tatC-gfp* were sufficient to complement the chain formation phenotype of the respective mutants (Fig. 3E and H). The vector pBAD-*tatA-gfp* had to be induced for complementation of the chain formation phenotype, indicating that more TatA-GFP is required for the functional Tat system than TatB-GFP or TatC-GFP (Fig. 3B). This result may simply reflect that in the natural Tat system the amount of TatA is much higher than that of TatB or TatC [2].

In recent years, it has become standard to test the functionality of the Tat system of *E. coli* physiologically by anaerobic growth on TMAO without a fermentable carbon source (e.g. [25]). Only cells with a functional Tat system can translocate the TMAO reductase (TorA) into the periplasmic space, thereby permitting growth on glycerol/TMAO minimal media under anaerobic conditions. We tested the TMAO respiration with a constitutive system. As shown in Fig. 4, TatB-GFP and TatC-GFP could support growth on TMAO. Growth of TatB- or TatC-deficient strains was significantly restored by pABS-*tatA*(*B-gfp*)*C* and pABS-tatAB(*C-gfp*), respectively, whereas the empty vector could not restore

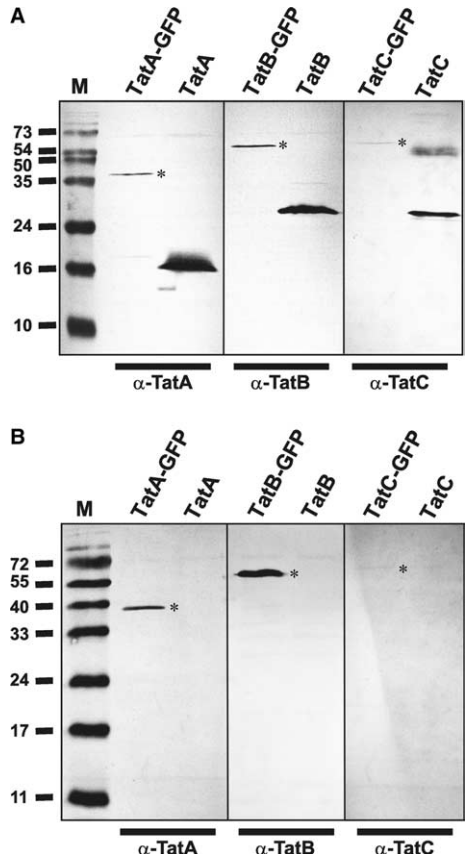

Fig. 2. Western blot detection of GFP fusion proteins. Membrane protein (11 μg) from strains expressing *tat-gfp* fusions or wild type *tat* genes were separated by SDS–PAGE and blotted. In (A), the Tat-GFP fusions from strains carrying pABS-derived vectors are compared with the recombinant Tat proteins as expressed from pABS-*tatABC*. TatA-GFP: *tatAE* mutant strain JARV16 with pABS-*tat(A-gfp)BC*; TatA: MC4100 with pABS-*tatABC*; TatB-GFP: *tatB* mutant strain BϕD with pABS-*tatA*(*B-gfp*)*C*; TatB: MC4100 with pABS-*tatABC*; TatC-GFP: *tatC* mutant strain B1LK0 with pABS-*tatAB*(*C-gfp*); TatC: MC4100 with pABS-*tatABC*. In (B), the Tat-GFP fusions from strains carrying pBAD-derived vectors are compared with the level of corresponding Tat proteins in MC4100 with the empty vector pBAD22. TatA-GFP: *tatAE* mutant strain JARV16 with pBAD-*tatA-gfp*; TatA: MC4100 with pBAD22; TatB-GFP: *tatB* mutant strain BϕD with pBAD-*tatB-gfp*; TatB: MC4100 with pBAD22; TatC-GFP: *tatC* mutant strain B1LK0 with pBAD-*tatC-gfp*; TatC: MC4100 with pBAD22. The blots were developed with antibodies recognizing TatA, TatB, or TatC, as indicated below the corresponding blots. M: marker-lane; Tat-GFP fusion proteins are labeled with asteriks. The diffuse band at about 55 kDa in the TatC (rec.) lane (A) is due to TatC aggregation in the heating step prior to loading.

growth. In the case of TatB-GFP, constitutive expression from pABS-*tatA(B-gfp)C* resulted in a chain formation phenotype. As TatB-GFP complemented the chain formation phenotype in the pBAD-system, it is obviously not a malfunction of TatB-GFP which causes the induction of cell chains with the pABS-based system. We believe that the cell chains form simply due to excess TatB-GFP at the cell poles, which somehow interferes with the cell division machinery. Strains containing pABS-*tatA*(*B-gfp*)*C* or pABS-*tatAB*(*C-gfp*) retained their GFP-fusion during TMAO respiration and formed by TMAO respiration on solidified media single colonies which contained the full length GFP fusions, indicating that the TMAO-growth data with TatB-GFP and TatC-GFP are reliable. In contrast, the support of TMAO

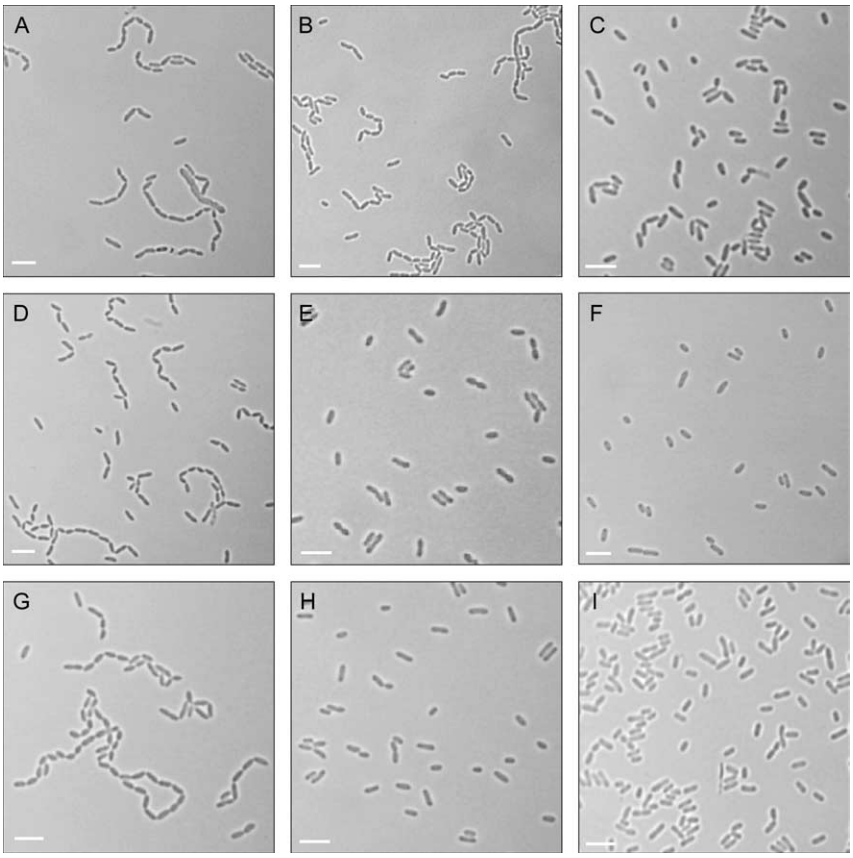

Fig. 3. Complementation of chain formation phenotype by Tat-GFP fusion proteins. Upper row: JARV16 with pBAD22 (A), pBAD-*tatA-gfp* uninduced (B), and pBAD-*tatA-gfp* induced with 0.1% arabinose (C). Middle row: BϕD with pBAD22 (D), pBAD-*tatB-gfp* uninduced (E), and pBAD-*tatB-gfp* induced with 0.1% arabinose (F). Lower row: B1LK0 with pBAD22 (G), pBAD-*tatC-gfp* uninduced (H), and pBAD-*tatC-gfp* induced with 0.1% arabinose (I).

respiration by TatA-GFP could not be unequivocally established, as we found that fluorescence-deficient derivatives were frequently formed, making long-term growth experiments with constitutive *tatA-gfp* expression impossible. We also noted that freshly transformed pABS-*tat*(*A-gfp*)*BC* containing clones formed larger and often deformed and highly fluorescent cells which rapidly reverted to lower fluorescent and less deformed derivatives with mainly polar fluorescence (data not shown). We therefore show for TatA-GFP only fluorescence data obtained with pBAD-*tatA-gfp*, which did not cause aberrant cell morphologies.

As a third line of evidence for functionality, we analyzed quantitatively the effect of the presence of TatA-GFP, TatB-GFP and TatC-GFP on SDS-sensitivity (Fig. 5). It has been described as one phenotype of Tat deficiency that the bacteria lose their natural resistance towards the ionic detergent SDS [26]. When the *tat-gfp* fusions were expressed by the pBAD system induced with 0.1% arabinose, we could establish that TatA-GFP restores SDS-resistance in the corresponding mutant strain (Fig. 5A). This positive result together with the complementation of the chain formation phenotype (Fig. 3) indicates that TatA-GFP is functional. In contrast, TatB-GFP and TatC-GFP, although functional in TMAO respiration and chain formation complementation, did not cure the SDS-sensitivity of the respective mutant strains (Fig. 5B and C). This might be due to unspecific effects on membrane stability by the recombinant membrane proteins.

4. Discussion

This study reports the first cellular localization analysis of the twin-arginine translocation system. GFP has been proven to be a valuable tool to analyze the localization of membrane proteins within bacterial cells [27,28]. Based on the concentration of Tat-GFP fusions at the cell poles (Fig. 1), we propose that the described 600 kDa TatABC complex [5] is not homogeneously distributed in the cytoplasmic membrane. The concentration of TatB-GFP at the cell poles is so far the strongest evidence for a polar localization of the translocon. TatC appears to be concentrated at the cell poles as well, an observation which is in perfect agreement with the existence of a TatBC complex. However, as the TatC-GFP fluorescence is very low we think that the TatC data must be regarded as first evidence only. TatA-GFP is abundant all over the membrane but also seems to be more concentrated at the poles in many cells. The distributions of TatA-GFP and TatB-GFP differ strongly, as TatA-GFP is abundant in the whole membrane, whereas TatB-GFP is restricted to distinct spots at the cell poles or at division planes of dividing cells. This suggests that most TatA and TatB are not interacting in stable complexes. TatA may diffuse freely in the membrane, in complexes such as the described 460 kDa TatA complex [6], whereas complexes containing TatB may be restricted to certain spots, usually located at the cell poles. The presence of polar fluorescence with TatC-GFP constructs fits to the observation that TatC

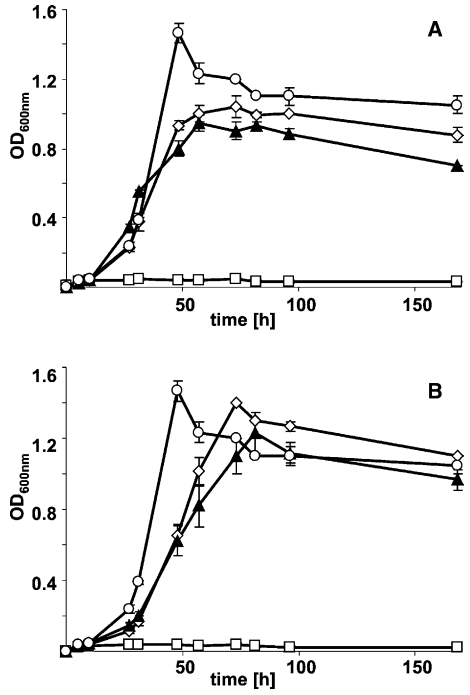

Fig. 4. TatB-GFP and TatC-GFP support TMAO respiration. (A) Growth of BϕD with pABS-*tatA(B-gfp)C* (filled triangles), pABS (squares), pABS-*tatABC* (diamonds) and MC4100 with pABS-*tatABC* (circles). (B) Growth of B1LK0 with pABS-*tatAB*(*C-gfp*) (filled triangles), pABS (squares), pABS-*tatABC* (diamonds) and MC4100 with pABS-*tatABC* (circles). The data points correspond to mean values from three independent cultures with standard deviations as indicated.

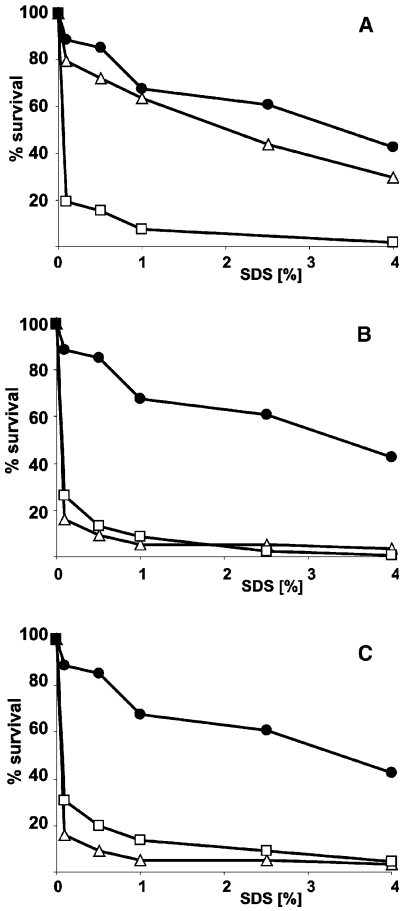

Fig. 5. Complementation of the SDS-sensitivity of Tat mutant strains by Tat-GFP fusions. SDS-sensitivity was quantified according to [26]. Briefly, liquid LB medium containing various concentrations of SDS was inoculated with exponentially growing arabinose-induced (0.1%, 3 h) cultures to a starting $OD_{600\ nm}$ of 0.05 and the $OD_{600\ nm}$ of the cultures was measured after 3 h of aerobic growth at 37 °C. The optical density of the culture in medium containing no SDS was defined as 100% survival. (A) SDS-sensitivity of the *tatAE* deficient strain JARV16 containing pBAD-*tatA-gfp* (triangles). (B) SDS-sensitivity of the *tatB* deficient strain BϕD containing pBAD-*tatB-gfp* (triangles). (C) SDS-sensitivity of the *tatC* deficient strain B1LK0 containing pBAD-*tatC-gfp* (triangles). All mutant strains were also tested with the empty vector pBAD22 (sensitivity control, squares) and compared with the wild type strain MC4100 with pBAD22 (resistance control, filled circles). The average error of data points as determined by this method was approximately 8%.

interacts with TatB [5]. As TatB and TatC are essential for translocation, it is likely that translocation actually takes place where TatB and TatC are located. TatA may freely diffuse in the membrane but assemble to the TatBC complex when the Tat substrate is bound – that would be in agreement with the current functional models of the Tat system. It has been clearly shown for the thylakoid Tat system that the translocon is not a rigid pore, but rather a substrate-induced assembly of TatA with a TatBC complex [29]. Even TatB and TatC might not always form a complex, as TatC may bind Tat substrates prior to TatB [8]. Thus, the detection of freely diffusing Tat system components – which could be involved in acquisition of Tat substrates – is not surprising. The targeting of Tat components to the poles may require interactions with cytoskeleton structures or with other proteins which contribute to the polarity of the cells, such as the Min system [30].

The expression systems we used resulted in functional Tat-GFP fusions and their fluorescence can therefore be taken as evidence for the localization of the respective natural translocon subunits. As the western blot analysis showed that the expression level was increased relative to the natural level, one cannot exclude that expression affects localization. However, in the case of the clearly polar localization of TatB-GFP, we do not see any reason why this TatB-GFP should be specifically targeted to the poles if not by a natural mechanism. Moreover, the polar localization fits with the polar appearance of GFP-fused Tat substrates. Micrographs from cells with Tat dependently translocated GFP show a fluorescent halo with stronger intensity at the cell poles, suggesting that Tat substrates enter the periplasm at the poles (Fig. 1 and [20–23]). Therefore, we think that the fluorescence data of translocon and substrate GFP-fusions together point to a polar localization of the functional translocon.

As to the question why the translocon is targeted to the cell poles, we think that the localization of the Tat components could be understood in the light of functional aspects. The Tat system may play a role in processes which take place at the cell poles, such as cell division or cell growth. Evidence for such a hypothesis might come from the fact that AmiA and AmiC, two amidases involved in cell division, are Tat substrates [23]. The polar assembly of translocon structures could also have mechanistic reasons: It is conceivable that the cell can more easily translocate folded proteins at its termini, possibly due to stabilizing interactions with protein partners at the cell poles. Surely, the localization of the Tat system opens a new per-

spective on functional and mechanistic aspects in this still fascinating field.

Acknowledgements: We thank Timothy Yahr and Matthias Müller for their generous donation of antisera. We are also very grateful to Tracy Palmer for sending us her *tat* deletion strains. We are indebted to Carsten Sanders and Tim Yahr for donation of plasmids. We thank Ute Lindenstrauss for excellent technical assistance, Anja Ebert for support with LSM techniques, Silke Trautmann for interest and fruitful communication, and Theresa Wermann for reading the manuscript. We especially thank Jan R. Andreesen for discussions and support. This work was supported by the Fonds der Chemischen Industrie and by the Deutsche Forschungsgemeinschaft (BR2285/1-1).

References

[1] Robinson, C. and Bolhuis, A. (2001) Protein targeting by the twin-arginine translocation pathway. Nat. Rev. Mol. Cell Biol. 2, 350–356.
[2] Palmer, T. and Berks, B.C. (2003) Moving folded proteins across the bacterial cytoplasmic membrane. Microbiology 149, 547–556.
[3] Sargent, F., Bogsch, E.G., Stanley, N.R., Wexler, M., Robinson, C., Berks, B.C. and Palmer, T. (1998) Overlapping functions of components of a bacterial Sec-independent protein export pathway. J. Biol. Chem. 274, 36073–36082.
[4] Sargent, F., Gohlke, U., De Leeuw, E., Stanley, N.R., Palmer, T., Saibil, H.R. and Berks, B.C. (2001) Purified components of the *Escherichia coli* Tat protein transport system form a double-layered ring structure. Eur. J. Biochem. 268, 3361–3367.
[5] Bolhuis, A., Mathers, J.E., Thomas, J.D., Barrett, C.M. and Robinson, C. (2001) TatB and TatC form a functional and structural unit of the twin-arginine translocase from *Escherichia coli*. J. Biol. Chem. 276, 20213–20219.
[6] Porcelli, I., de Leeuw, E., Wallis, R., van den Brink-van der Laan, E., de Kruijff, B., Wallace, B.A., Palmer, T. and Berks, B.C. (2002) Characterization and membrane assembly of the TatA component of the *Escherichia coli* twin-arginine protein transport system. Biochemistry 41, 13690–13697.
[7] De Leeuw, E., Granjon, T., Porcelli, I., Alami, M., Carr, S.B., Müller, M., Sargent, F., Palmer, T. and Berks, B.C. (2002) Oligomeric properties and signal peptide binding by *Escherichia coli* Tat protein transport complexes. J. Mol. Biol. 322, 1135–1146.
[8] Alami, M., Luke, I., Deitermann, S., Eisner, G., Koch, H.G., Brunner, J. and Müller, M. (2003) Differential interactions between a twin-arginine signal peptide and its translocase in *Escherichia coli*. Mol. Cell 12, 937–946.
[9] Casadaban, M.J. (1976) Transposition and fusion of the *lac* genes to selected promoters in *Escherichia coli* using bacteriophage lambda and Mu. J. Mol. Biol. 104, 541–555.
[10] Sargent, F., Stanley, N.R., Berks, B.C. and Palmer, T. (1999) Sec-independent protein translocation in *Escherichia coli*: a distinct and pivotal role for the TatB protein. J. Biol. Chem. 274, 36073–36082.
[11] Bogsch, E.G., Sargent, F., Stanley, N.R., Berks, B.C., Robinson, C. and Palmer, T. (1998) An essential component of a novel bacterial protein export system with homologues in plastids and mitochondria. J. Biol. Chem. 273, 18003–18006.
[12] Englesberg, E., Anderson, R.L., Weinberg, R., Lee, N., Hoffee, P., Huttenhauer, G. and Boyer, H. (1962) L-Arabinose-sensitive, L-ribulose 5-phosphate 4-epimerase-deficient mutants of *Escherichia coli*. J. Bacteriol. 84, 137–146.
[13] Overmann, J., Fischer, U. and Pfennig, N. (1992) A new purple sulfur bacterium from saline littoral sediments *Thiorhodovibrio winogradskyi* gen. nov. and sp. nov.. Arch. Microbiol. 157, 329–335.
[14] Brüser, T., Yano, T., Brune, D.C. and Daldal, F. (2003) Membrane targeting of a folded and cofactor-containing protein. Eur. J. Biochem. 270, 1211–1221.
[15] Sanders, C., Wethkamp, N. and Lill, H. (2001) Transport of cytochrome c derivatives by the bacterial Tat protein translocation system. Mol. Microbiol. 41, 241–246.
[16] Cormack, B.P., Valdivia, R.H. and Falkow, S. (1996) FACS-optimized mutants of the green fluorescent protein (GFP). Gene 173, 33–38.
[17] Lowry, O.H., Rosebrough, N.J., Farr, A.L. and Randall, R.J. (1951) Protein measurement with the Folin phenol reagent. J. Biol. Chem. 193, 265–275.
[18] Laemmli, U.K. (1970) Cleavage of structural proteins during the assembly of the head of bacteriophage T4. Nature 227, 680–685.
[19] Brüser, T., Deutzmann, R. and Dahl, C. (1998) Evidence against the double-arginine motif as the only determinant for protein translocation by a novel Sec-independent pathway in *Escherichia coli*. FEMS Microbiol. Lett. 164, 329–336.
[20] Santini, C.L., Bernadac, A., Zhang, M., Chanal, A., Ize, B., Blanco, C. and Wu, L.F. (2001) Translocation of jellyfish green fluorescent protein via the Tat system of *Escherichia coli* and change of its periplasmic localization in response to osmotic up-shock. J. Biol. Chem. 276, 8159–8164.
[21] Ize, B., Gerard, F. and Wu, L.F. (2002) In vivo assessment of the Tat signal peptide specificity in *Escherichia coli*. Arch. Microbiol. 178, 548–553.
[22] Thomas, J.D., Daniel, R.A., Errington, J. and Robinson, C. (2001) Export of active green fluorescent protein to the periplasm by the twin-arginine translocase (Tat) pathway in *Escherichia coli*. Mol. Microbiol. 39, 47–53.
[23] Bernhardt, T.G. and de Boer, P.A. (2003) The *Escherichia coli* amidase AmiC is a periplasmic septal ring component exported via the twin-arginine transport pathway. Mol. Microbiol. 48, 1171–1182.
[24] Yahr, T.L. and Wickner, W.T. (2001) Functional reconstitution of bacterial Tat translocation in vitro. EMBO J. 20, 1–8.
[25] Gouffi, K., Santini, C.L. and Wu, L.F. (2002) Topology determination and functional analysis of the *Escherichia coli* TatC protein. FEBS Lett. 525, 65–70.
[26] Ize, B., Stanley, N.R., Buchanan, G. and Palmer, T. (2003) Role of the *Escherichia coli* Tat pathway in outer membrane integrity. Mol. Microbiol. 48, 1183–1193.
[27] Chen, J.C., Weiss, D.S., Ghigo, J.M. and Beckwith, J. (1999) Septal localization of FtsQ, an essential cell division protein in *Escherichia coli*. J. Bacteriol. 181, 521–530.
[28] Sievers, J. and Errington, J. (2000) The *Bacillus subtilis* cell division protein FtsL localizes to sites of septation and interacts with DivIC. Mol. Microbiol. 36, 846–855.
[29] Mori, H. and Cline, K. (2002) A twin arginine signal peptide and the pH gradient trigger reversible assembly of the thylakoid [Delta]pH/Tat translocase. J. Cell. Biol. 157, 205–210.
[30] Errington, J., Daniel, R.A. and Scheffers, D.J. (2003) Cytokinesis in bacteria. Microbiol. Mol. Biol. Rev. 67, 52–65.
[31] Guzman, L.M., Belin, D., Carson, M.J. and Beckwith, J. (1995) Tight modulation, regulation and high-level expression by vectors containing the arabinose P_{BAD} promoter. J. Bacteriol. 177, 4121–4130.